SEVENTH EUROPEAN ROTORCRAFT AND POWERED LIFT AIRCRAFT FORUM

PAPER N°46

APPLICATION OF THE ONERA DYNAMIC STALL MODEL TO A HELICOPTER BLADE IN FORWARD FLIGHT

C.T. TRAN[1] D. FALCHERO[2]

[1] Office National d'Etudes et de Recherches Aérospatiales 92320 Châtillon - F -
[2] Société Nationale Industrielle Aérospatiale 13722 Marignane - France -

September 8 - 11, 1981

Garmisch-Partenkirchen
Federal Republic of Germany

Deutsche Gesellschaft für Luft- und Raumfahrt e. V.

Goethestr. 10, D-5000 Köln 51, F.R.G.

APPLICATION OF THE ONERA DYNAMIC STALL MODEL TO A HELICOPTER BLADE IN FORWARD FLIGHT

by C.T. Tran[1] and D. Falchero[2]

[1] Office National d'Etudes et de Recherches Aérospatiales (ONERA)
92320 Châtillon (France)

[2] Société Nationale Industrielle Aérospatiale (SNIAS)
13722 Marignane (France)

ABSTRACT

The ONERA Semi-Empirical Model for the 2-D Dynamic Stall of Airfoils presentedat the 6th European Rotorcraft and Powered-lift Aircraft Forum has been applied to the case of a helicopter rotor system in forward flight.

The paper describes both aspects of stability and periodic response :

. Form of the Floquet modes-subharmonic oscillation and almost periodic oscillation,
. Evolution of these modes as functions of the rotor advance ratio,
. Periodic response and aerodynamic force and moment,
. Comparison with a Quasi-Steady aeroelastic calculation showing the effects of unsteady phenomena.

INTRODUCTION

The methods employed at ONERA for the analysis of the rotary wing aeroelasticity are drawn from the linear principles involving, for the aerodynamic field, the 3-D acceleration potential lifting surface theory (1.2), and for the structural dynamics, the modal representation of partial modes characterising separately the helicopter blade and fuselage (3).

At high flight speeds of the rotorcraft, aimed by the helicopter industry, the linear analysis ceases to be valid. Since as a consequence of high speeds, the rotor retreating blade can penetrate locally in the regions of dynamic stall, while the rotor advancing blade tip is submitted to unsteady transonic shock wave effects. Such aerodynamic non-linearities can only be treated, on theoretical grounds, by the general equations of fluid mechanics.

For engineering purpose, ONERA, in collaboration with the SNIAS and the CEAT, have recently made considerable effort in establishing a semi-empirical 2-D dynamic stall model (4.5) in order to represent the dynamic stall characteristics of an airfoil section. This paper describes the 1st attempt in the application of the cited model to the case of a helicopter blade in forward flight.

Though relatively simple compared with the real complex phenomenon of rotor blade dynamic stall, the unsteady time derivatives of force and moment involved in the model introduce in the blade dynamic equations additional aerodynamic degrees of freedom (what is termed as "hidden" D.O.F. in mechanical vibrations).

The presence of these aerodynamic D.O.F. originates, from the necessity to simulate, by the model, the time history effects of the fluid flow. These additional aerodynamic D.O.F., added to the structural D.O.F., lead to the final form of the aeroelastic equations of the form of a large set of linearized differential equations with periodic coefficients.

The difficulty of a large system of equations is avoided in this first application by considering a simplified rotor system where there is no gyroscopic coupling between blades and the rotor hub. The single blade analysis is further simplified by assuming the blade to be rigid in both flap and lead lag, but is only torsionally elastic. The structural variables are then the rigid blade flapping angle and the torsion mode generalized coordinates. It is believed that this simplified scheme for the rotor system is sufficient to describe phenomena such as stall flutter and subharmonic oscillation as recorded by helicopter flight tests.

This paper presents both aspects of stability and periodic response :

. Form of the Floquet modes -subharmonic and almost periodic oscillations,

. Evolution of these modes as a function of the rotor advance ratio,

. Comparison with quasi-steady aeroelastic calculations showing the effects of unsteady phenomena.

1. Kinematics of a blade element

The kinematics of a blade element will be described by the superposition of mouvements composed of the advancing flight velocity V_∞ of the helicopter, the angular velocity of rotation Ω of the rotor, the rotation of the angle β of the rigid blade flapping motion, the rotation of the angle θ of the blade's collective & cyclic pitches, and the elastic deflection of the blade sections in torsional deformation ϕ.

Let S (i j k) be an orthonormal base (fig. 1). The origin of S, coincident with the centre of the rotor hub, advances at the uniform flight velocity $\mathbf{V}_\infty$, while the vector of rotation $\boldsymbol{\Omega}$ lies constantly along the k axis, inclining at a rotor shaft tilt angle ($90^\circ - \Lambda$) with $\mathbf{V}_\infty$. With respect to a fixed reference system :

$$\mathbf{V}_\infty = \mathbf{S} \begin{pmatrix} -V_\infty \sin\Lambda \\ 0 \\ V_\infty \cos\Lambda \end{pmatrix}$$

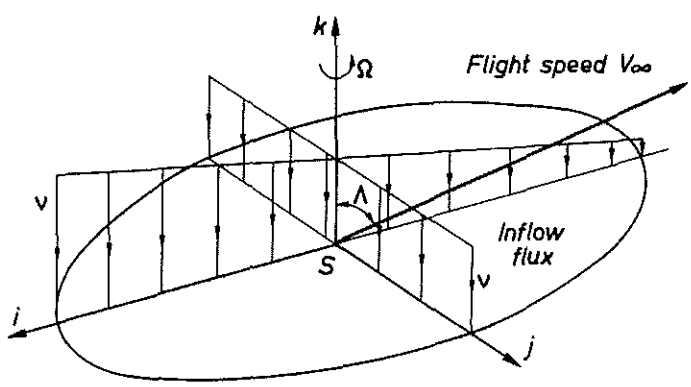

Fig. 1 : Rotor system in forward flight

The following orthogonal transformations of bases will be carried out in order to express conveniently the blade element coordinates.

S_1 $(i_1 j_1 k_1)$ is obtained by rotating S through a finite angle $(\psi(t) - \pi/2)$ about k.

S_2 $(i_2 j_2 k_2)$ is obtained first by rotating S_1 through an angle $\beta(t)$ about i_1, then by displacing its origin through a distance y_0 along j_1.

S_3 $(i_3 j_3 k_3)$ is obtained first by rotating S_2 through a finite angle $\alpha(t)$ about j_2, then by displacing its origin through a distance y_p along j_2.

S_1, S_2, S_3 are related, for all vectors, by the orthogonal rotation matrices :

$$S_3 = S_2 k_3 \; ; \; S_2 = S_1 k_2 \; ; \; S_1 = S K_1$$

with

$$k_1 = \begin{pmatrix} \sin\psi & \cos\psi & 0 \\ -\cos\psi & \sin\psi & 0 \\ 0 & 0 & 1 \end{pmatrix} \qquad k_2 = \begin{pmatrix} 1 & 0 & 0 \\ 0 & \cos\beta & -\sin\beta \\ 0 & \sin\beta & \cos\beta \end{pmatrix} \qquad k_3 = \begin{pmatrix} \cos\alpha & 0 & \sin\alpha \\ 0 & 1 & 0 \\ -\sin\alpha & 0 & \cos\alpha \end{pmatrix}$$

From figure 2, one identifies that $\psi = \Omega t$ (Ω = constant) and $\beta(t)$ (=O(1) ; 1st order small quantity) are respectively the blade's azimuthal position and flapping angle. $\alpha = \theta(t) + \bar{\nu}(y) + \phi(y, t)$ is the local instantaneous angle (composed of the cyclic & collective pitches $\theta(t)$, blade twist $\bar{\nu}(y)$, and torsional deflection $\phi(y, t)$ (=O(1)) between the tangent to a blade section and the rotor tip-path plane $(i_2 j_2)$.

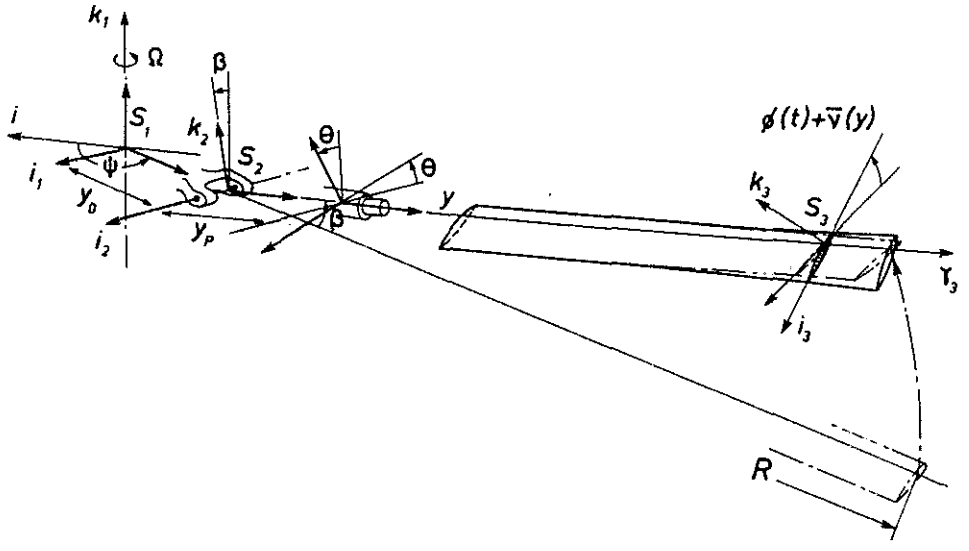

Fig. 2 : Simplified helicopter rotor system

The local bases S_3 are everywhere coincident with the local blade section tangents. In admitting that the blade torsional deflection induces no variation in length to its longitudinal neutral fibre, the position vector of a blade element is expressed by its local cartesian coordinates :

$$P = S_3 \begin{pmatrix} x \\ y \\ 0 \end{pmatrix}$$

Referring to the fixed coordinate system S :

$$P = S\begin{pmatrix} -V_\infty t \sin\Lambda \\ 0 \\ V_\infty t \cos\Lambda \end{pmatrix} + SK_1 \left\{ K_2 \left\{ K_3 \begin{pmatrix} x \\ y \\ 0 \end{pmatrix} + \begin{pmatrix} 0 \\ y_p \\ 0 \end{pmatrix} \right\} + \begin{pmatrix} 0 \\ y_0 \\ 0 \end{pmatrix} \right\}$$

The velocity is then obtained by differentiation. Expressing in the rotating reference system S_1, the velocity V of a blade element is then :

$$V = \dot{P} = S_1 \bar{K}_1 \begin{pmatrix} -V_\infty \sin\Lambda \\ 0 \\ V_\infty \cos\Lambda \end{pmatrix} + S_1 \begin{Bmatrix} -\Omega(r\cos\beta + y_0) - x\sin\alpha(\Omega\sin\beta + \dot{\theta} + \dot{\phi}) \\ x\cos\alpha(\Omega + \sin\beta(\dot{\theta} + \dot{\phi})) - \dot{\beta}(r\sin\beta - x\sin\alpha\cos\beta) \\ -x\cos\alpha\cos\beta(\dot{\theta} + \dot{\phi}) + \dot{\beta}(r\cos\beta + x\sin\alpha\sin\beta) \end{Bmatrix} \quad (1)$$

with $r = y + y_p$

1.1 - Model representation

The blade's elastic torsional deformation will be expressed by a modal superposition. Let $\phi_i(y)$ be the spatial function defining the torsional deflection mode shapes of the blade cantilevered on a non-rotating fixed hub, and $s_i(t)$ the generalized coordinates. ϕ is then written as :

$$\phi(y, t) = \sum_i^m \phi_i(y)\, s_i(t) = \bar{\phi}\, s$$

With $\bar{\phi}$ the line-vector of elements ϕ_i, and s the column vector of elements s_i. One will designate henceforth γ as the diagonal generalized rigidity matrix, of elements $\gamma_{ii} = w_i^2 \mu_{ii}$; where μ_{ii} are the diagonal elements of the generalized mass matrix μ :

$$\mu_{ii} = \iint x^2 \phi_i \phi_i \, dm$$

and w_i the corresponding torsional modal circular frequency.

2. Equations of motion

Let q (t) the column, of dimension n = m + 1, of the generalized coordinates :

$$\bar{q} = (\beta, \bar{s})$$

The Lagrange equations written in terms of the coordinates q are given by :

$$\frac{d}{dt}\frac{\partial \mathcal{T}}{\partial \dot{q}} - \frac{\partial \mathcal{T}}{\partial q} + \frac{\partial U}{\partial q} + \frac{\partial D}{\partial \dot{q}} = Q$$

where $\mathcal{T}$, U and D are respectively the kinetic energy, potential energy and the dissipation function of the system integrated over all the blade elements :

$$\mathcal{T} = \frac{1}{2}\iint \bar{V} V \, dm \quad , \quad U = \frac{1}{2}\bar{s}\gamma s$$

and Q represents the column of the generalized aerodynamic forces of unsteady lift and pitching moment.

It is assumed that the dissipation arising from the structural damping will be negligible compared with that originated from the aerodynamic forces. The dissipation function D will therefore not be taken into account.

Application of the Lagrange equations, retaining only terms of the 1st order leads to the following system of 2nd order differential equation :

$$M(t)\ddot{q} + B(t)\dot{q} + K(t)q = f(t) + Q(t, q, \dot{q}, \ddot{q}) \tag{2.1}$$

$$M = \begin{array}{|c|c|} \hline \iint (r^2 + x^2 \sin\theta)\, dm & -\iint r x \cos\theta \bar{\phi}\, dm \\ \hline -\iint r x \cos\theta \phi\, dm & \mu \\ \hline \end{array} \tag{2.2}$$

$$B = 2\Omega \begin{array}{|c|c|} \hline & -\iint x \sin^2\theta \bar{\phi}\, dm \\ \hline \iint x \sin^2\theta \phi\, dm & \\ \hline \end{array} \tag{2.3}$$

$$K = \Omega^2 \begin{array}{|c|c|} \hline \iint (r^2 + r y_o - x^2 \sin^2\theta)\, dm & -\iint (r + y_o) x \cos\theta \bar{\phi}\, dm \\ \hline -\iint (r + y_o) x \cos\theta \phi\, dm & \gamma/\Omega^2 + \iint x^2 \cos 2\theta \phi \bar{\phi}\, dm \\ \hline \end{array} \tag{2.4}$$

$$f = \begin{pmatrix} \iint x (\ddot{\theta} r \cos\theta + 2\Omega x \dot{\theta} \sin^2\theta + \Omega^2 (r + y_o) \sin\theta)\, dm \\ -\iint x^2 (\ddot{\theta} + \Omega^2 \sin\theta \cos\theta)\, \phi\, dm \end{pmatrix} \tag{2.5}$$

One notes that the M, B, K are periodic matrices having the same periodicity as the input cyclic pitch. Though they conserve the usual forms of a gyroscopic system :

$M = \bar{M}$, and $\forall q \neq 0$, $\bar{Q}MQ > 0$
$B = -\bar{B}$ and $\bar{Q}BQ = 0$, or purely imaginary number
$K = \bar{K}$, the classical stability criteria cannot be applied to the homogeneous systems (2.1), since these matrices are not constant in time.

All the present stage, it seems that the periodic coefficients appearing in M, B, K may not be eliminated, neither by a type of multi-bladed coordinate transformation, nor by refereing the position variables with respect to a particular reference frame. In any case, it appears that there is no need to try to eliminate these coefficients, since, as will be shown later the unsteady aerodynamic forces will themselves introduce extra variable coefficients.

$$Q = \int_{\text{blade}} (C_N W + C_M \Phi)\, dy \qquad (7.1)$$

where

$$W = \frac{1}{2}\rho c V^2(r,t)\begin{pmatrix} r\cos\theta(t) \\ 0 \end{pmatrix}, \quad \Phi = \frac{1}{2}\rho c^2 V^2(r,t)\begin{pmatrix} 0 \\ \phi(y) \end{pmatrix} \qquad (7.2)$$

with

$$V^2 = \left(\Omega(y_0 + r) + V_\infty \sin\Lambda \sin\Psi\right)^2 + \left(V_\infty \cos\Lambda + \nu\right)^2$$

3. Non-linear unsteady aerodynamics

The non-linear unsteady aerodynamics presently adopted is based on the "Semi-Empirical Model For The Dynamic Stall Of Airfoils In View Of The Application To The Calculation Of Responses of A Helicopter Blade In Forward Flight", ref. (5), developed recently by ONERA. The model concerns an airfoil section executing forced oscillation in pitch in 2-D flow. Physical considerations and arguments based on experimental observations both on the time history effect of the flow and on the evolution of the responses in the frequency domain, led to the establishing of functional relationships relating The input variables (incidence, angular pitch rate, mach number, and their time derivatives) and the output variables (Overall lift and pitching moment coefficients and their time derivatives). These functional relationships are in the form of two differential equations of the 3rd order with variable coefficients. The coefficients of the equations are then determined, for a given airfoil, by identification of the test results of the 2-D airfoil in static and in small amplitude harmonic oscillation or random vibration configurations. The model has been applied to cases of large amplitude oscillations in pitch of the same airfoil and comparisons of the predicted lifts and moments with those of the experimental results were satisfactory.

Application of the model to the case of a helicopter blade in forward flight presents some difficulties :

- The variable coefficients of the model's equations depend on the local Mach number, and on the local aerodynamic incidence of the airfoil section ; the latter being partly unknown a priori.

- The unsteady Mach number effect arising from the resolved in-plane component of the helicopter forward flight velocity.

- Combined motions of blade flap, cyclic pitch and blade torsional elastic deformation.

One will assume the hypothesis of the quantitative equivalence between the unsteady aerodynamic characteristics resulting from the blade's vertical heaving and pitching motions. In fact, the experimental results of reference (7) indicated clearly the validity of this hypothesis in the helicopter operating range of frequencies and amplitudes. The effects of these two types of motion will therefore be superimposed, as has been done in deriving the 2-D aerodynamic incidence (eqn. 6).

One will further assume that the variation of the blade local Mach number may be regarded as quasi-steady, since this variation is essentially due to the in-plane 1 per rev. resolved component of the flight velocity, and thus is of low frequency. However, in this first application, one will, for simplification, regard the Mach number as constant (M = 0.3).

2.1 Generalized aerodynamic forces

As in the classical 2-D strip theory, it is admitted that the rotor aerodynamic flow field may be considered as two-dimensional for all local blade sections.

Let's consider, figures 2 and 3, an elementary blade section of length dy, inclined at an angle α with respect to the i_2 axis. The aerodynamic forces per unit length of both lift L, and pitching moment M (respectively of coefficients C_N and C_M), act at the blade's fore-quarter chord section (x = 0). The positive directions of these forces are taken conventionally as indicated in fig. 3. Let P = P (q,t) the position vector of this fore-quarter chord point, $\boldsymbol{\alpha}(t)$ the rotation vector of the blade section, and n = n (q, t) the unit vector normal to the blade section. F, M, and their respective coefficients C_N and C_M are classically related by :

$$\boldsymbol{F} = \tfrac{1}{2}\rho V^2 c\, C_N \boldsymbol{n} \quad , \quad \boldsymbol{M} = \tfrac{1}{2}\rho V^2 c^2 C_M \boldsymbol{j}_3$$

where C is the chord, ρ the fluid density and V (t) is the instantaneous local 2-D velocity at point P, limited to the order 0.

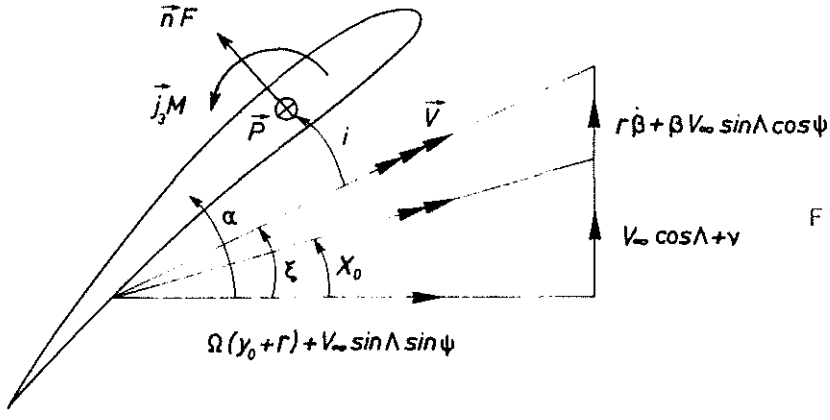

Fig. 3 : 2-D airfoil section aerodynamic incidence i

The virtual work $\delta\omega$ is then expressed by

$$\delta\omega = \int_{\text{blade}} (\delta\bar{\boldsymbol{P}}\boldsymbol{F} + \delta\bar{\boldsymbol{\alpha}}\boldsymbol{M})\, dy$$

Now $$\delta\bar{\boldsymbol{P}}\boldsymbol{n} = \delta\bar{q}\,\frac{\partial\bar{\boldsymbol{V}}}{\partial\dot{q}}\boldsymbol{n} + \delta\bar{\boldsymbol{V}}\boldsymbol{n}\,\delta t = \delta\bar{q}\,\frac{\partial v_n}{\partial\dot{q}} + \delta v_n\,\delta t$$

and $$\delta\bar{\boldsymbol{\alpha}} = \left(\delta\bar{q}\,\frac{\partial\alpha}{\partial q} + \frac{\partial\alpha}{\partial t}\,\delta t\right)\boldsymbol{j}_3$$

where $v_n = \bar{\boldsymbol{V}}\boldsymbol{n}$ is the local normal velocity to the blade section at P. It has been found that n does not depend on $\dot{q}$.

The generalized aerodynamic force Q of equation (2.1) is then :

$$\boldsymbol{Q} = \tfrac{1}{2}\int \rho V^2 c \left(\frac{\partial v_n}{\partial\dot{q}} C_N + c\,\frac{\partial\alpha}{\partial q} C_M\right) dy \qquad (4)$$

2.2 2-D aerodynamic incidence

The 2-D aerodynamic incidence can be defined by considering the various local 2-D velocities in planes containing the airfoil sections.

In forward flight, the total flux penetrating the rotor disk consists of firstly, the normal component of the flight velocity $V_\infty \cos\Lambda$ of the helicopter and secondly, of the inflow flux, of induced velocity ν which, by virtue of the momentum theory, maintains the equilibrium of the rotor lift and weight. The expression for ν presently adopted is given by reference (6) :

$$\nu(y_0+r,\psi) = \nu_0\left(1+\frac{y_0+r}{R}\tan\frac{\chi}{2}\cos\psi\right)$$

where ν_0 is the mean induced velocity, given as a function of the rotor mean lift F_0 :

$$\nu_0 = \frac{F_0}{2\pi V_\infty \rho R^2}$$

and χ is the skew wake angle defined as $\tan^{-1}\left(\frac{V_\infty \sin\Lambda}{\nu_0}\right)$.

Remark : In specifying a blade pitch input, and in adopting such an inflow model implies a priori a trim condition for the rotor blades. The pitch input may be specified for instance by a flight test, and the trim condition must be checked a posteriori when all calculations are done.

The inflow of induced velocity ν will be described in the base S This, added to expression (1), leads to the fore quarter chord point velocity V in the blade tip-path plane, base S_2 :

$$V = S_2\begin{pmatrix} -\Omega(y_0+r) - V_\infty \sin\Lambda \sin\psi \\ -V_\infty \sin\Lambda\cos\psi + \beta(V_\infty\cos\Lambda+\nu) \\ \beta V_\infty \sin\Lambda\cos\psi + r\dot{\beta} + V_\infty\cos\Lambda+\nu \end{pmatrix} + 0\ (2) \qquad (4)$$

The unit vector normal to a blade section is given by :

$$n = S_2\begin{pmatrix}\sin\alpha\\0\\\cos\alpha\end{pmatrix}$$

and hence the blade section normal velocity :

$$v_n = \bar{V}n = -\sin\alpha\,(\Omega(y_0+r) + V_\infty \sin\Lambda \sin\psi + \cos\alpha\,(\beta V_\infty \sin\Lambda \cos\psi + r\dot{\beta} + V_\infty\cos\Lambda + \nu) \qquad (5)$$

The 2-D local aerodynamic incidence i is defined by the angle between the 2-D local blade section velocity (equation 4, neglecting the radial flow velocity), and the tangent to the blade section (fig. 3). We have :

$$\bar{V}n = -|V||n|\sin i$$

In comparing with (5), one obtains for i :

$$i = \alpha - \xi \qquad (6)$$

with

$$\xi = \tan^{-1}\left(\frac{V_\infty\cos\Lambda + \nu + r\dot{\beta} + \beta V_\infty \sin\Lambda\cos\psi}{\Omega(y_0+r) + V_\infty\sin\Lambda\sin\psi}\right)$$

From (3) and (5), the column of the generalized aerodynamic forces is expressed by :

The model's equations are given in reference (4,5) the normal lift coefficient C_N, and the pitching moment coefficient C_M, are each expressed by the sum of two functions :

$$C_N = C_{N1} + C_{N2} \quad (8.1) \qquad C_M = C_{M1} + C_{M2} \quad (8.2)$$

These functions are governed by the following differential equations :

$$\dot{C}_{N1} + \lambda_N C_{N1} = \lambda_N \left(C_{N0\ell} + \Delta_N \dot{\alpha} \right) + \delta_N \frac{di}{dt} + \Delta_N \ddot{\alpha} \qquad (8.3)$$

$$\ddot{C}_{N2} + B_N \dot{C}_{N2} + K_N C_{N2} = - K_N \left(\Delta C_{N0} + e_N \frac{d}{dt} \Delta C_{N0} \right) \qquad (8.4)$$

$$\dot{C}_{M1} + \lambda_M C_{M1} = \lambda_M \left(C_{M0\ell} + \Delta_M \dot{\alpha} \right) + \delta_M \frac{di}{dt} + \Delta_M \ddot{\alpha} \qquad (8.5)$$

$$\ddot{C}_{M2} + B_M \dot{C}_{M2} + K_M C_{M2} = - K_M \left(\Delta C_{M0} + e_M \frac{d}{dt} \Delta C_{M0} \right) \qquad (8.6)$$

The symbol ($\dot{}$) designates differentiation with respect to the physical time t, i is the 2-D local aerodynamic incidence defined by (6)

And $B_N = 2 \alpha_N \gamma_N$, $B_M = 2 \alpha_M \gamma_M$

$K_N = \gamma_N^2 (1 + \alpha_N^2)$, $K_M = \gamma_M^2 (1 + \alpha_M^2)$

With, respectively :

$\lambda_N(i)$, $\lambda_M(i)$	lift and moment delay parameters
$C_{N0\ell}(i)$, $C_{M0\ell}(i)$	lift and moment linear static curves, extended up to the incidence i in consideration
$\pm j\gamma_N(i)$, $\pm j\gamma_M(i)$	complex poles of the 2nd order systems
$\alpha_N(i)$, $\alpha_M(i)$	reduced damping coefficients associated with the complex poles
$\Delta C_{N0}(i)$, $\Delta C_{M0}(i)$	functions represent, for an incidence i, respectively the difference between the linear static curve and the true stati curve of lift and moment.
	the remaining coefficients represent, in a small amplitude $\tilde{\theta}$ sinusoidal motion, respectively :

$\Delta_N \tilde{\theta}$, $\Delta_M \tilde{\theta}$ slopes of the imaginary part of the lift and moment at high frequency, $\delta_N \tilde{\theta}$, $\delta_M \tilde{\theta}$ asymptotes of the real part of lift and moment, e_N, e_M parameters determining the phase shifts of the excitations, and α (t) represents the angular coordinate (geometric pitch) of the airfoil section with respect to the blade tip-path plane.

Remark C_{N1} and C_{N2}, (respecitvely C_{M1} and C_{M2}) may be eliminated by combining equations 8.1, 8.3 and 8.4, (respectively 8.2, 8.5 and 8.6). This procedure will result in a single 3rd order equation for C_N, (respectively C_M).

Equations (8) are non-linear with respect to the incidence i, which is a function of the generalized coordinate q.

From (6), $i = \alpha - \varphi$

with $\varphi = \tan^{-1} (X_0 + X_1)$

where $X_0 = \dfrac{V_\infty \cos\Lambda + \nu}{\Omega(y_c + r) + V_\infty \sin\Lambda \sin\psi} = O(0)$, $X_1 = \dfrac{\dot{r\beta} + \beta V_\infty \sin\Lambda \cos\psi}{\Omega(y_0 + r) + V_\infty \sin\Lambda \sin\psi} = o(1)$

The development of φ about X_0 leads to :

$$i = \tilde{\alpha} + \epsilon \tag{9.1}$$

where $$\tilde{\alpha}(r,t) = \theta(t) + \bar{\nu}(y) - \tan^{-1}\left(X_0(r,t)\right) \quad = 0 \ (0) \tag{9.2}$$

and $$\epsilon(q,r,t) = \phi(r,t) - \frac{1}{1+X_0^2(r,t)}\, X_1(r,t,\beta,\dot{\beta}) \quad = 0 \ (1) \tag{9.3}$$

The system (8) may, at any instant, be linearized about the variable $\tilde{\alpha}(r,t)$ the known part of the aerodynamic incidence. However, the linearisation scheme is valid only if the linearisation distances ϵ (q,r,t) remain small at all time, which is generally not the case for the retreating blade's inboard sections. Nevertheless, the problem may be solved iteratively as follows :
From (9.1), one writes :

$$i = (\tilde{\alpha} + \Delta\epsilon) + (\epsilon - \Delta\epsilon) \tag{10}$$

The system (8) will now be linearized about $(\tilde{\alpha} + \Delta\epsilon)$,
where $\Delta\epsilon$ take on the values of ϵ resulting from previous successive calculations.

Remark : Computational experience indicates that except for high advance ratios where dynamic stall is predominant, the rigid blade flapping motion β is relatively insensitive to unsteady effects. Thus the iteration can be initiated by a non-time consuming quasi-steady calculation. From (9.3) and (10), it is seen the linearisation distances :

$$(\epsilon - \Delta\epsilon) \sim (\phi - \phi_{QS}) \ll 1$$

where ϕ_{QS} is the torsional deflection derived from a quasi-steady calculation. Since the difference between two torsional deflections (resulting from 2 successive calculations) is usually small, the solutions converge, again, except for high advance ratios, in one single iteration.

The system (8) linearized about $(\tilde{\alpha} + \Delta\epsilon)$ leads to :

$$\begin{aligned}
&\dot{C}_{N1} + \lambda_N C_{N1} = f_{N1} + R_{N1} q + S_{N1} \dot{q} + T_{N1} \ddot{q} \\
&\ddot{C}_{N2} + B_N \dot{C}_{N2} + K_N C_{N2} = f_{N2} + R_{N2} q + S_{N2} \dot{q} + T_{N2} \ddot{q} \\
&\dot{C}_{M1} + \lambda_M C_{M1} = f_{M1} + R_{M1} q + S_{M1} \dot{q} + T_{M1} \ddot{q} \\
&\ddot{C}_{M2} + B_M \dot{C}_{M2} + K_M C_{M2} = f_{M2} + R_{M2} q + S_{M2} \dot{q} + T_{M2} \ddot{q}
\end{aligned} \tag{11}$$

where the forcing terms f_{N1} and f_{N2} are given by :

$$f_{N1}(r,t) = \lambda_N \left(C_{N0\ell} + \delta_N \dot{\theta} - \frac{\partial C_{N0\ell}}{\partial \theta} \Delta\epsilon \right) + \delta_N \ddot{\theta}$$

$$f_{N2}(r,t) = -K_N \left(\Delta C_{N0} - \frac{\partial \Delta C_{N0}}{\partial \theta} \left(e_N \dot{\tilde{\alpha}} + \Delta\epsilon \right) \right)$$

And similarly for f_{M1} and f_{M2} by writing the subscript M in place of N .

The aerodynamic rigidity, damping and inertial terms are given by :

$$R_{N1}(r,t) = \left(V_\infty \sin\Lambda \left(\Omega \delta_N z \sin\psi - \left(\delta_N \dot{z} + \lambda_N \frac{\partial C_{N0\ell}}{\partial \theta} z \right) \cos\psi \right),\ \lambda_N \frac{\partial C_{N0\ell}}{\partial \theta} \bar{\phi} \right)$$

$$S_{N1}(r,t) = \left(-\delta_N Z V_\infty \sin\Lambda \cos\psi - \delta_N r\dot{z} - \lambda_N \frac{\partial C_{N0l}}{\partial\theta} rZ \,,\; (\lambda_N \Lambda_N + \delta_N)\bar{\Phi} \right)$$

$$T_{N1}(r,t) = \left(-\delta_N rZ \,,\; \Lambda_N \bar{\Phi} \right)$$

$$R_{N2}(r,t) = \left(V_\infty \sin\Lambda K_N \frac{\partial \Delta C_{N0}}{\partial\theta} (Z\cos\psi + e_N \dot{z}\cos\psi - \Omega e_N Z \sin\psi), - K_N \frac{\partial \Delta C_{N0}}{\partial\theta}\bar{\Phi} \right)$$

$$S_{N2}(r,t) = \left(K_N \frac{\partial \Delta C_{N0}}{\partial\theta} (e_N Z V_\infty \cos\psi + rZ + e_N r\dot{z}), - K_N e_N \frac{\partial \Delta C_{N0}}{\partial\theta} \bar{\Phi} \right)$$

$$T_{N2}(r,t) = \left(K_N e_N \frac{\partial \Delta C_{N0}}{\partial\theta} rZ \,,\; 0 \right)$$

where $Z = \left(\Omega (y_c + r) + V_\infty \sin\Lambda \sin\psi \right) / V^2$

R_{M1}, S_{M1}, T_{M1}, R_{M2}, S_{M2} and T_{M2} can similarly be obtained by writing the subscript M in place of N.

4. Final form of the dynamic equations

Consider the equations of motion (2) and (7). The blade spanwise integration of the generalized forces is performed by the Graussian numerical integration, and the system (2) reads :

$$M(t)\ddot{q} + B(t)\dot{q} + K(t)q = f(t) + \sum_{k=1}^{K} H_k(\eta_k) \left(C_{Nk}(\eta_k,t) W_k(\eta_k,t) + C_{Mk}(\eta_k,t) \Phi(\eta_k,t_i) \right)$$

where η_k is the reduced abscissa of the k^{th} spanwise integration point and H_k is the corresponding weighting function.

The lift coefficient $C_{Nk} = C_{N1k} + C_{N2k}$, and the moment coefficient $C_{Mk} = C_{M1k} + C_{M2k}$, at each integration point k, are given by the set of equations (11).

Let X be the state vector, of elements q, $\dot{q}/\Omega^*$ and the set of aerodynamic coefficients defined on K total integration points :

$$\bar{X} = \left(\bar{q}, \bar{\dot{q}}/\Omega^*, \ldots\ldots, \underbrace{C_{N1k}, C_{N2k}, \dot{C}_{N2k}/\Omega^*, C_{M1k}, C_{M2k}, \dot{C}_{M2k}/\Omega^*}_{k^{th}\text{ integration point}} \ldots\ldots \right) \qquad (12)$$

Ω^* being a normalisation angular frequency which is a priori arbitrary.

The dimension of X being L = 2n + 6K.

The global system is brought then to a set of L differential equations of the 1st order : $M(t) + B(t) = G(t)$

with

$$\bar{G} = \left(0, \bar{f}/\Omega^*, \ldots\ldots, \underbrace{f_{N1k}, 0, f_{N2k}/\Omega^*, f_{M1k}, 0, f_{M2k}/\Omega^*}_{k^{th}\text{ integration point}}, \ldots\ldots \right)$$

The global system of dynamic equations is moreover expressed in a more classical form :

$$\dot{X} + A(t)X = F(t) \qquad (13)$$

with $A(t) = M^{-1}B$, square matrix of the L^{th} order, perdiodic in time t of period $\mathcal{T} = 2\pi/\Omega$. And F (t) a column vector periodic with the periodicity as A.

$$\mathcal{B} =$$

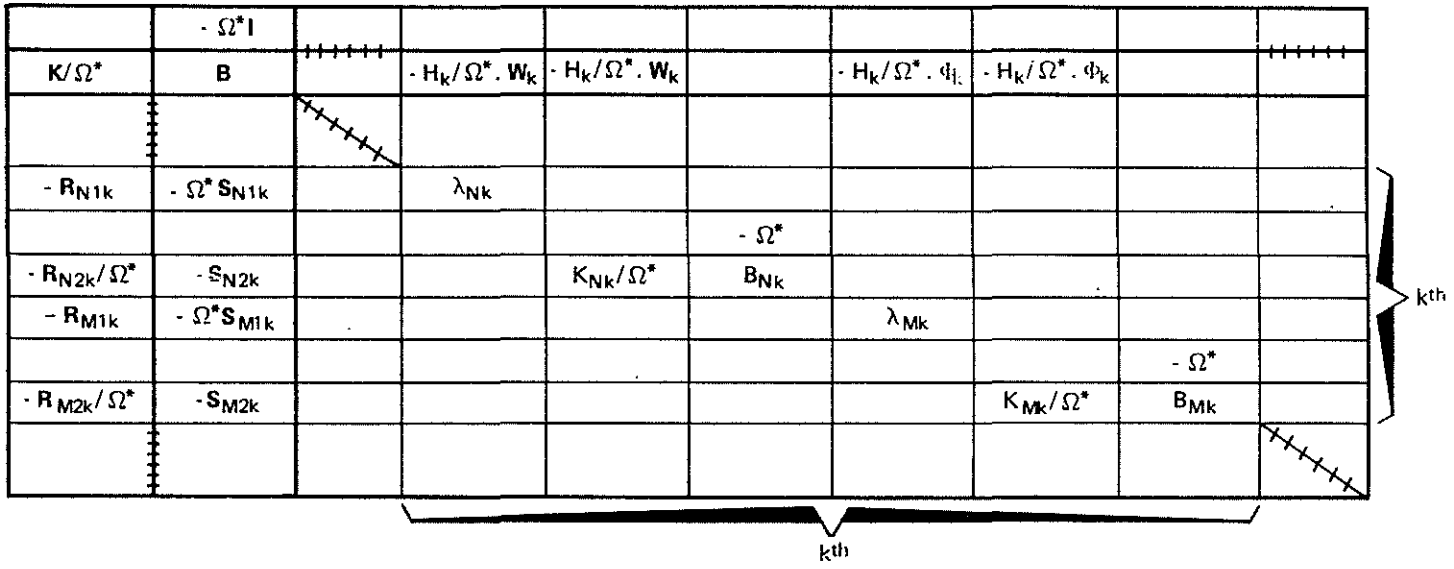

$$\mathcal{M} =$$

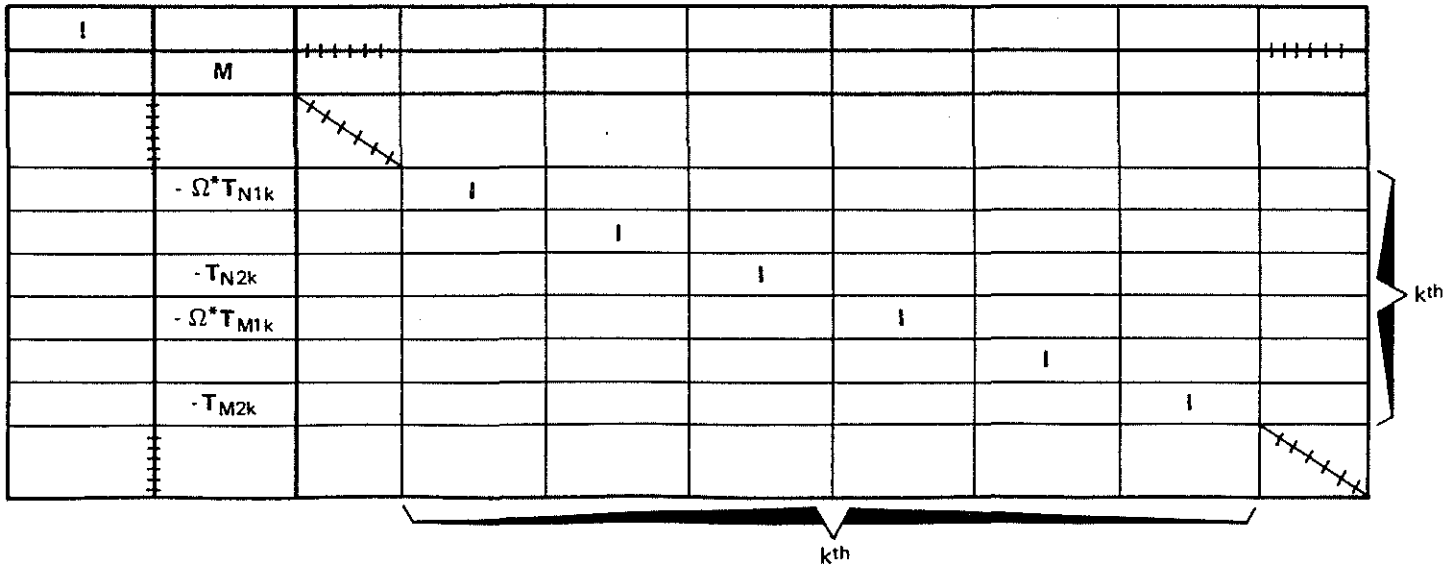

Remark : In most aeroelastic problems, the aerodynamic forces are either given by the classical 2-D quasi-steady strip theory, or in the linear case, by the Duhamel's superposition integrals of the Küssner's and the Wagner's functions (reference 8), the aerodynamic forces can be written explicitly in both cases. The aeroelastic coupling therefore introduces no extra aerodynamic degrees of freedom (D.O.F.).

In the present report however, the aerodynamic model being in the form of differential equations with coefficients dependent on the local 2-D incidence, no procedure apparently can be applied to eliminate these extra D.O.F. The situation is seemingly similar to that in mechanical vibrations where the structures possess hidden D.O.F. Elimination of these hidden D.O.F., if possible, is usually achieved by carrying the structural variables to their "augmented state", i.e. by augmenting the order of the governing differential equations.

5. Resolution

5.1 Stability and Floquet modes

The stability of the homogeneous set of equations (13) is studied by the Floquet's theory, of which a brief review is given here in in order to define more precisely the form of the FLoquet modes.

Consider the homogeneous set (13) :

$$\dot{X} + A(t)X = 0 \tag{14}$$

Let $Z(t)$ be the non singular matrix, called "the transition matrix", formed by L independent solutions of (14) : $(X_1 \ldots\ldots X_L)$. Z verifies :

$$\dot{Z} + A(t)Z = 0$$

$A(t)$ being periodic of period ζ , it can be shown that :

$$Z(t+\zeta) = Z(t)C \tag{15}$$

where C is non singular, and is defined by :

$$C = \exp(B\zeta)$$

and hence

$$B = 1/\zeta \log\left(Z^{-1}(0)Z(\zeta)\right) \tag{16}$$

The system (14) is reducible in the sense of Liapunov, as, by introducing the periodic matrix L, of period ζ :

$$L(t) = Z(t)\exp(-Bt) \tag{17}$$

The transformation

$$X(t) = L(t)Y(t) \tag{18}$$

applies to (14) leads to the system of equations with constant coefficients :

$$\dot{Y} - BY = 0 \tag{19}$$

with $B = -L^{-1}(\dot{L} + AL)$

Assuming the general case where B is semi-simple, let $\boldsymbol{\lambda}$ and U be respectively the diagonal matrix of eigen-values and the matrix of eigen-vectors of B :

$$B = U \boldsymbol{\lambda} U^{-1}$$

In comparing with (16), one identifies that $\boldsymbol{\Lambda} = \exp(\boldsymbol{\lambda} \tau)$ and U are respectively the diagonal matrix of eigen-values and the matrix of eigen-vectors of $(\mathbf{Z}^{-1}(0)\,\mathbf{Z}(\tau))$.

The eigen-values λ_j of the matrix B, which are called the characteristic exponents of the periodic matrix A (t), are given by :

$$\alpha_j = \Re(\lambda_j) = 1/\tau \log |\Lambda_j| \tag{20.1}$$

$$\omega_j = \Im(\lambda_j) = 1/\tau \left(\theta_j \pm 2k\pi\right) \tag{20.2}$$

with $$\theta_j = \tan^{-1}\left(\frac{\Im(\Lambda_j)}{\Re(\Lambda_j)}\right) \tag{20.3}$$

The stability criteria of the system (19), and hence of the original system (14), is defined by :

$$\Re(\lambda_j) \leq 0 \quad , \text{or} \quad |\Lambda_j| \leq 1$$

From (16), (17) and (18), the set of L transient solutions of the system (14) can be written as :

$$\begin{aligned} \mathbf{X}(t) &= \mathbf{Z}(t)\mathbf{Z}^{-1}(0)\mathbf{X}(0) \\ &= \mathbf{L}(t)\mathbf{U}\exp(\boldsymbol{\lambda} t)\mathbf{U}^{-1}\mathbf{Z}^{-1}(0)\mathbf{X}(0) \end{aligned}$$

By adopting the initial values Z (o) U for X (o), one obtains :

$$\begin{aligned} \mathbf{X}(t) &= \mathbf{Z}(t)\mathbf{U} \\ &= \mathbf{L}(t)\mathbf{U}\exp(\boldsymbol{\lambda} t) \end{aligned} \tag{21.1}$$

Thus the j^{th} solution :

$$\mathbf{X}_j(t) = \mathbf{Z}(t)\mathbf{U}_j = \mathbf{L}(t)\mathbf{U}_j e^{\lambda_j t} \tag{21.2}$$

The X_j are called the Floquet modes of the periodic system (14), reference (9). These being so-called since substitution of (21.1) in the system (14) results in the classical eigen-value problem of expression (19).

The matrix $(\mathbf{Z}^{-1}(0)\,\mathbf{Z}(\tau))$ being real, its eigen-values are then real or complex conjugated pairs. Referring to expressions (20), complex conjugated pairs of eigen-values Λ give rise also to complex conjugated pairs of λ and U of the matrix B, and these can be combined to form a real Floquet mode :

$$\begin{aligned} \mathbf{X}_j(t) &= \mathbf{Z}(t)\left(\mathbf{U}_j + \mathbf{U}_j^*\right) \\ &= 2\,e^{\alpha_j t}\mathbf{L}(t)\,\Re\left(\mathbf{U}_j e^{i\omega_j t}\right) \end{aligned} \tag{21.3}$$

As for real eigen-values Λ_j, two cases are to be considered :

— $\Re(\Lambda_j) > 0$, $\Im(\Lambda_j) = 0$; and hence $\theta_j = 0$, $\omega_j = \pm k\Omega$. The X_j remains real, as it should be, by combination of the two conjugated solutions :

$$\begin{aligned} \mathbf{X}_j(t) &= 2\,\mathbf{Z}(t)\mathbf{U}_j \\ &= 2\,e^{\alpha_j t}\mathbf{L}(t)\mathbf{U}_j\,\Re(e^{ik\Omega t}) \end{aligned} \tag{21.4}$$

— $\Re(\Lambda_j) < 0$, $\Im(\Lambda_j) = 0$; $\theta_j = \pm\pi$, and $\omega_j = \pm\frac{\Omega}{2}(1+2k)$ are equally solutions, and these can also be combined to form a real Floquet mode :

$$X_j(t) = 2\,Z(t)\,U_j$$
$$= 2\,e^{\alpha_j t} L(t)\,U_j\,\mathcal{R}\left(e^{i\frac{\Omega}{2}(1+2k)}\right) \qquad (21.5)$$

Remark : It is noted that the indetermination of ω_j due to the additive factor $2k\pi$ (20.2) has no consequence on the definition of the Floquet modes ; these being defined implicitly by the first terms of expressions (21.3, 21.4, 21.5).

In constant coefficient differential equations, the modes are characterised by eigen-solutions of the form :

$$X_j(t) = e^{\alpha_j(t)}\,\mathcal{R}\left(U_j\,e^{i\omega_j t}\right)$$

with U_j constant eigen-vectors. The undamped modal wave forms are thus constants or sinusoidal functions of time. The undamped Floquet modal wave forms, however, exhibit various time-varying features depending on the eigen-values Λ , or λ :

- $\mathcal{R}(\Lambda_j) > 0$, $\mathcal{J}(\Lambda_j) = 0$; From (21.4)

The undamped wave forms are periodic functions of time, of frequency Ω equal to the rotor rotational circular frequency Ω .

- $\mathcal{R}(\Lambda_j) < 0$, $\mathcal{J}(\Lambda_j) = 0$

From (21.5),

The undamped wave forms are periodic functions of time, of frequency $\Omega/2$ equal to half of the rotor rotational circular frequency Ω , irrespective of the indetermination of the additive factor $2k\pi$.

There are thus "subharmonic oscillations of frequency $\Omega/2$.

- Λ_j purely imaginary pairs ;

From (20.2), $\omega_j = \pm \frac{\Omega}{4}(1 + 4k)$. The undamped wave forms again exhibit "subharmonic oscillations" of frequency $\Omega/4$ equal to a quarter of the rotor rotational circular frequency Ω , irrespective of the indetermination of the additive factor $2k\pi$.

- General case of Λ_j complex conjugated pairs ;

From (21.3), the undamped wave forms are given by the sums of a number (finite or infinite) of terms of periodic functions resembling those of Fourier Series. However, the frequencies of these periodic functions are not rational ratios, and hence their periodicities have no largest common integral factor. The sums of such periodic functions are therefore not periodic. The undamped Floquet modal wave forms are then ever-changing in time, with no repetitive patterns.

There are thus "almost periodic oscillations".

Lastly, as for the transient effect, it is seen from (21.1) that X (0) = L (0) U ; and X ($n\zeta$) = L (0) U exp ($n\zeta$), by the periodicity of L .

Hence :
$$X_j(n\zeta) = X_j(0)\,e^{\lambda_j n\zeta} = X_j(0)\,\Lambda_j^{n}$$

Thus each j^{th} Floquet mode changes by a factor Λ_j from period to period.

5.2 Evolutions of the modal characteristics as function of advance ratio

Classically, evolutions of the modal characteristics, frequencies ω_j, and damping α_j as a function of the advance ratio μ, are traced by observing their continuities for successive small increments of μ. In the present problem, the large number of degrees of freedom, originating essentially from the application of the ONERA 2-D Dynamic Stall Modal, renders the tracking by this means particularly difficult.

However, precise definition of these evolutions is essential ; firstly to define the stability envelope, and secondly to determine the additive factor $2k\pi$ in ω_j (20.2), thus allowing to express the Floquet modes in more convenient analytical forms. It is proposed here to outline a method to trace more efficiently the evolutions of these modal characteristics. The method is based on consideration of continuities of the eigen-vectors, for successive small increments of μ.

Consider the set of linearly independent eigen-vectors U_j, corresponding to the eigen-values λ_j of the matrix B, for a given advance ratio μ.

Define the space metric K such that :

$$< U_i , U_j > = U_i^+ K U_j = \delta_{ij}$$

where the symbols (+) and δ_{ij} denote respectively the complex conjugate transpose and the Kronecker delta.
We have :

$$U^+ K U = I \quad , \text{ and } K = (U U^+)^{-1}$$

K is hermitan, positive definite, and the set of vectors U_j is K-orthogonal.

For small increment $\Delta\mu$ of the advance ratio, let $V_i = U_i + \Delta U_i$ be the new set of linearly independent eigen-vectors of the matrix $B + \Delta B$. We can, in principle, make each vector V_i of the new set to correspond to a single vector U_j of the original set. That is :

$$V_i \sim U_j \quad , \quad \Delta\mu/\mu \ll 1$$

$$\text{and } < V_i , U_j > \; = \; 1, \quad \Delta\mu \to 0 \quad ; \tag{22}$$

except for an arbitrary normalisation factor. It is noted that generally $i \neq j$, due to the arbitrary classification of eigen-vectors.

By extension of the geometrical concept of the angle between two real vectors, the "complex angle" α_{ij}, formed by two complex vectors V_i and U_j is defined by :

$$\cos(\alpha_{ij}) = \frac{< V_i , U_j >}{< V_i , V_i >^{1/2} < U_j , U_j >^{1/2}} \tag{23}$$

with $| \cos(\alpha_{ij}) | \leq 1$, by the Cauchy-Schwartz inequality. The complex number $\cos(\alpha_{ij})$ thus lies within the unit circle, and all arbitrary normalisation factors alter only its phase.

Equation (22) expresses the "parallelism" of two vectors, and equation (23) its degree of parallelism.

Continuous evolutions of the eigen-vectors, for small increments $\Delta\mu$, can then be determined by measuring the angles formed by each vector V_i of the new set and all the vectors U_j of the original set. The criteria of two vectors that are most K-parallel, and hence continuously evolved, is given by the $\underset{ij}{\text{Max}} \; | \cos(\alpha_{ij}) |$.

The situation may be readily illustrated, by analogy, by considering a 3-D Euclidean space.

5.3 Forced response and periodic solutions

Consider the non-homogeneous system (13), of which the formal solution is expressed by (reference 10) :

$$\mathbf{X}(t) = \mathbf{Z}(t)\,\mathbf{X}(0) + \int_0^t \mathbf{Z}(t)\,\mathbf{Z}^{-1}(\sigma)\,\mathbf{F}(\sigma)\,d\sigma \qquad (24)$$

With no loss of generality, $Z(0) = I$ has been imposed.

It is assumed that the homogeneous system (14) is stable, i.e. $\mathcal{R}(\lambda_j) \leq 0$ or $|\Lambda_j| \leq 1$, and it is proposed to determine the periodic solution of period $\mathcal{Z}$ of (13).

By imposing the periodicity condition : $X(\mathcal{Z}) = X(0)$, one obtains :

$$\mathbf{X}(0) = \mathbf{Z}(\mathcal{Z})\,\mathbf{X}(0) + \int_0^{\mathcal{Z}} \mathbf{Z}(\mathcal{Z})\,\mathbf{Z}^{-1}(\sigma)\,\mathbf{F}(\sigma)\,d\sigma$$

To obtain all periodic solutions of (13), one must solve, for X (0), the system :

$$\mathbf{X}(0) = \left(\mathbf{I} - \mathbf{Z}(\mathcal{Z})\right)^{-1} \int_0^{\mathcal{Z}} \mathbf{Z}(\mathcal{Z})\,\mathbf{Z}^{-1}(\sigma)\,\mathbf{F}(\sigma)\,d\sigma \qquad (25)$$

Provided that the system (14) has no periodic solution of period $\mathcal{Z}$, more precisely, provided that none of the eigen-values λ_j of the matrix B is zero, nor of the form $\pm i2k\pi/\mathcal{Z}$, equation (25) defines uniquely the initial conditions X (0). The periodic solution of the system (13) are then obtained by substitution of (25) in (24).

Remark : The transition matrix Z (t) is regular at all time, since $\det(Z(t)) = \exp\left(-\int_0^t tr(\mathbf{A}(\sigma))\,d\sigma\right)$, and trA being finite. However, this matrix is often ill-conditionned at low frequency Ω and hence at large t up to the period $\mathcal{Z}$. In fact, Z (t) decays rapidly due to the large aerodynamic pitching moment dissipation. This ill-condition leads to numerical inaccuracies in the inversion of Z (t), as is required in integrals such as (24).

Computational experience showed that Z (t) is best computed by subdividing t into elementary intervals :

$$t = t_n > t_{n-1} > \ldots\ldots > t_1 > t_0 = 0$$

And write

$$Z(t) \simeq \exp(C_n)\,\exp(C_{n-1})\ldots\ldots\exp(C_1)\,I, \qquad (26)$$

by the multiplicative rule of the transition matrix ;

with

$$\mathbf{C}_k = -\int_{t_k}^{t_{k+1}} \mathbf{A}(\sigma)\,d\sigma \simeq -\Delta t_k\,\mathbf{A}\left(\frac{t_k + t_{k+1}}{2}\right), \quad \Delta t_k = t_{k+1} - t_k$$

The convergence and the truncation error of the approximation (26) had been studied by (reference 11), and the efficiency of this approximation as

compared to a 4th order Runge-Kutta integration technique had also been shown by (reference 12).

The matrix exp (C_k) can be calculated directly from its definition :

$$\exp(C_k) = \sum_{m=0}^{\infty} \frac{C_k^m}{m!}$$

This being so, the inversion of the matrix Z (t) in integrals such as (24) may now be avoided, since the expression

$$Z(t)\,Z^{-1}(\sigma), \quad \text{with} \quad t = \sum_{k}^{n} \Delta t_k \,, \quad \sigma = \sum_{k}^{m} \Delta t_k \;; \quad n \geq m$$

is now :

$Z(t)\,Z^{-1}(\sigma) = \exp(C_n)\exp(C_{n-1}) \ldots\ldots \exp(C_1)\,I\,.\,I \exp(-C_1) \ldots\ldots \exp(-C_{m-1})\exp(-C_m) = \exp(C_n) \ldots\ldots \exp(C_{m+1})$
by commutativity of the matrices two by two.

6. Numerical results

The single blade analysis described in the previous sections has been applied to the case of a helicopter rotor in hover $\mu = 0$, and in forward flights, up to $\mu = 0.35$.

The rotor weight, geometry, velocities and control pitch inputs, and the blade's characteristics, correspond to the flight cases of a research helicopter of the SNIAS. The blade has been assumed to be rigid in both flap and lead-lag, but torsionally elastic, and is hinged to the rotor hub with a certain offset. The torsional deformation is based on the modal superposition of one single torsional mode of modal frequency 183 rd/s. The column vector q (section 2) is thus of dimension 2, of elements $\beta(t)$ the blade flap angle, and s (t) the torsional generalised coordinate.

The blade spanwise integration of the generalized aerodynamic forces has been performed with 5 Gaussian integration points. The dimension of the state vector X is thus 2 x 2 + 6 x 5. This then leads to a system of 34 non-homogeneous differential equations with periodic coefficients (equ. 13).

All calculations are initiated by a non time-consuming Q-S calculation for which the incidence is defined by (9.1). The Q-S equations are linearized about the known part $\tilde{\alpha}$, which will be termed as the linearized incidence. The resulting incidence $\tilde{\alpha} + \epsilon$ is then employed to linearize equations (8) as indicated in section (3).

6.1 Floquet modes

Figures (4) and (5) show the evolutions of the eigen-values $\lambda = \alpha + i\omega$ (equ. 20) of the blade flapping mode and the blade torsional mode, as a function of the rotor forward flight speed.

Starting with the hover case, where the governing equations (14) are of constant coefficients. The eigen-values are defined with no ambiguity. The rotor constant rotational circular frequency Ω being 39.5 rd/s, it is seen that the flapping mode frequency ω is dropped to 36 rd/s (instead of greater than Ω in vacuum), due to the aerodynamic damping and rigidity effects. The torsional mode frequency exhibits the same tendency.

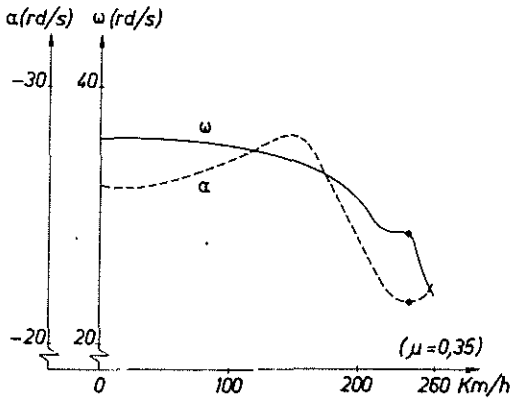

Fig. 4 : Frequency and damping of the blade flapping mode as a f_n of flight speed

Fig. 5 : Frequency and damping of the blade torsional mode as a f_n of flight speed.

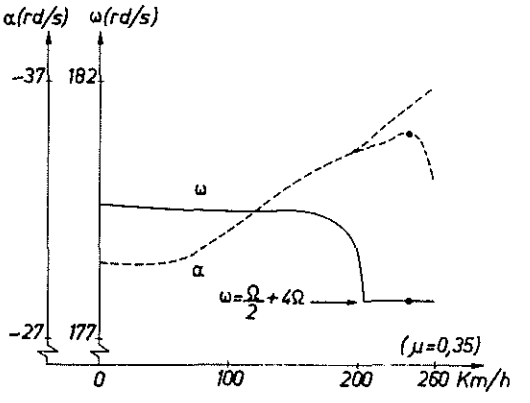

As μ increases, the eigen-values are traced by continuities of their corresponding eigen-vectors, by the method indicated in section (5.2). Some difficulties may be encountered in the tracking process in regions of frequency crossings, but these can readily be solved. The additive factors $2k\pi$ in the definition of ω are then determined by continuities of the eigen-values.

One particular aspect is shown in the evolution of the torsional mode. The eigen-values λ of the torsional mode, starting as a complex-conjugated pair, split up into two negative unequal roots, as from 200 km/h. These give rise to two eigen-solutions (equ. 21.5) of the same circular frequency $\omega = (\frac{\Omega}{2}+4\Omega)$, but of different damping coefficients α. The situation is analogous to that of constant coefficient differential equations when one pair of the conjugated eigen-values becomes real, except that in the latter case, the frequency is locked at the value zero over a certain interval of the parameter μ, whereas in the present Floquet modes, the frequency is locket at values that are odd multiples of $\frac{\Omega}{2}$, thus subharmonic oscillation of frequency $\frac{\Omega}{2}$. In both cases, there might be risk of instability, since the splitting of the eigen-values could eventually leads to positive damping coefficient.

Figures (6) and (7) show the undamped Floquet modal wave forms (equ. 21) as a function of time, from $t = 0$ up to $t = 3\zeta$ corresponding to a flight speed of 240 km/h ($\mu = 0.32$). It is noted that the transition matrix needs be calculated only from $t = 0$ up to the period ζ. The evolution in time of the Floquet modes at $t > \zeta$ can be obtained simply by use of equ. 15.

Figure 6 corresponds to one of the eigen-values of the torsional mode, and figure (7) that of the flapping mode. The flapping motion β, and the torsional generalized coordinate s, together with the aerodynamic degrees of freedom (D.O.F.), $C_N = C_{N1} + C_{N2}$ (normal lift coefficient), and $C_M = C_{M1} + C_{M2}$ (pitching

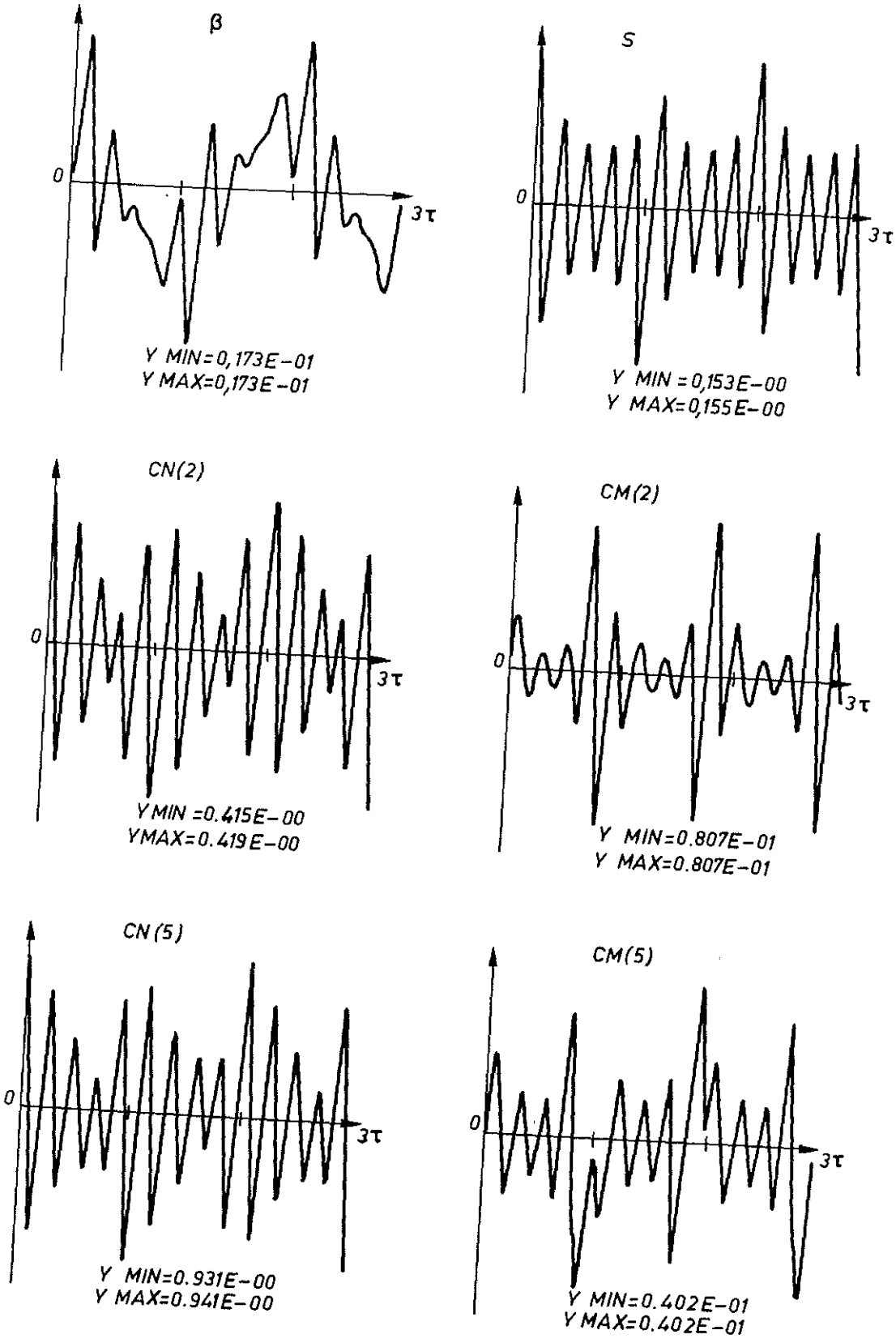

Fig. 6 : Undamped Floquet modal wave forms for the blade torsional mode.

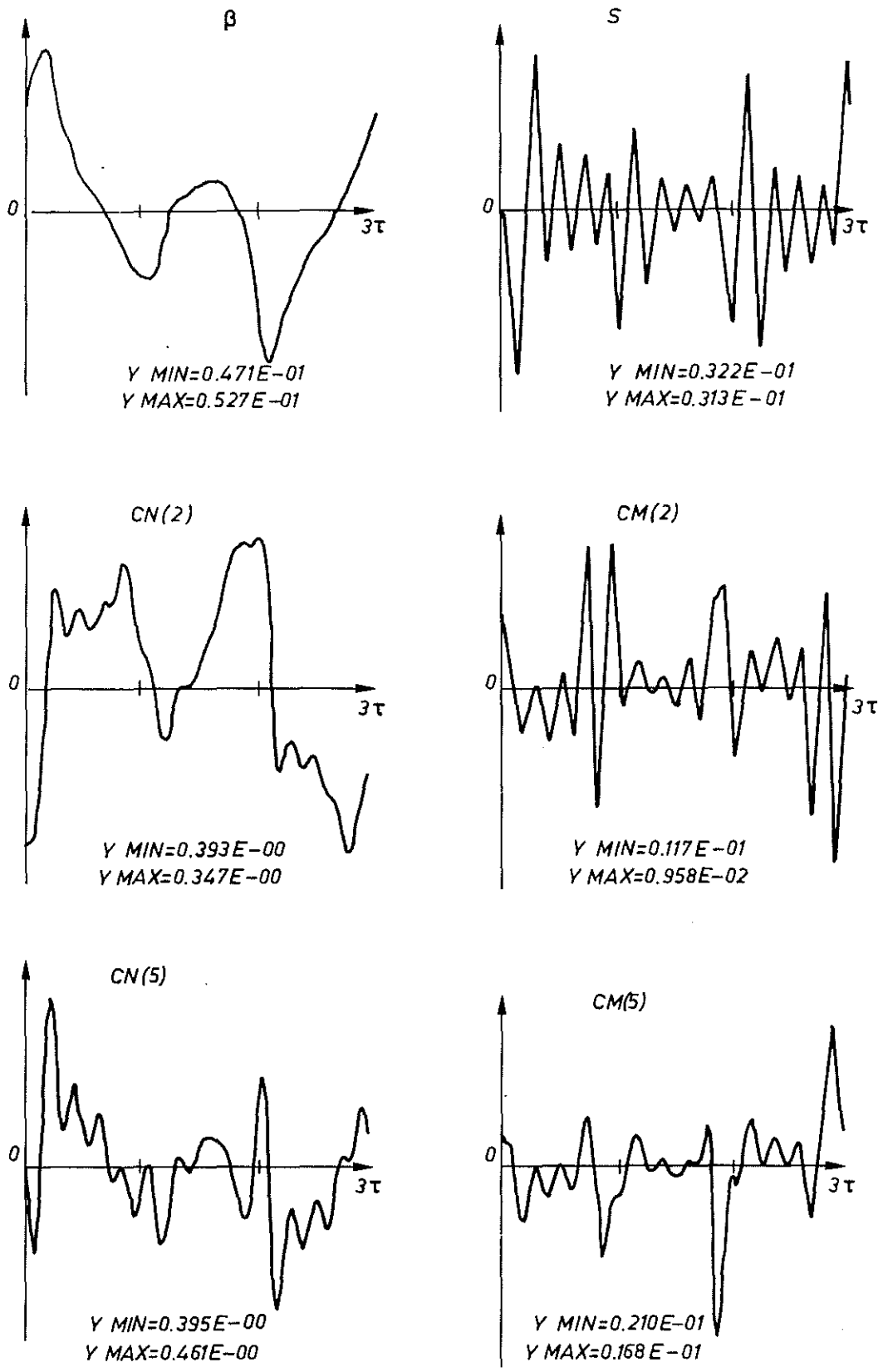

Fig. 7 : Undamped Floquet modal wave forms for the blade flapping mode

moment coefficient) at two spanwise blade sections : ($y_0 + r$)/R = 0.41 and 0.96 corresponding to the Gaussian integration points (2) and (5), are illustrated in both figures. As is mentioned, the torsional mode at this flight speed displays the character of subharmonic oscillations of frequency $\Omega/2$. It can be seen from fig. (6), that all variables illustrated are periodic functions of period equal to 2π, twice the rotor rotation period. It can also be remarked that all the wave forms have predominant $9\Omega/2$ frequency content, this being the frequency ω of the torsional mode. As for the blade flapping mode, whose frequency ω and Ω not being a ratio, it is seen from fig. (7) that all variables display almost periodic oscillation, with no definite repetitive pattern. In both cases, it is observed that there is non negligible participation of the aerodynamic D.O.F., due to strong aeroelastic couplings. As a matter of fact, at the flight speed considered, some of the aerodynamic mode frequencies are in close viscinity of those of the structural modes.

6.2 Periodic responses

The periodic responses of the system (13) have also been computed at the same flight speed of 240 Km/h.

Fig. (8.1) through fig. (8.8) show the evolutions of the periodic responses of β, δ, and for the two previous blade spanwise sections (2) and (5), the aerodynamic incidence i, the aerodynamic normal lift force F, and the aerodynamic pitching moment M, for both the quasi-steady (Q-S) and the unsteady calculations.

Referring first to figs. (8.3) and (8.4) for incidences i, the broken lines represent the linearized incidences about which the Q-S equations are linearized. The incidences resulting from the Q-S calculation are represented by the dotted lines, about which the unsteady equations (8) are then linearized. The solid lines represent the incidences issued from the unsteady calculation. It is seen that for both blade sections, the differences between the Q-S and the unsteady incidences are everywhere small, thus the unsteady calculation is regarded to have converged in one single iteration. The same remark may be applied to the Q-S calculation. This then allows to compare the two calculations, and hence to illustrate the unsteady effects.

In comparing the flapping responses β resulting from the two calculations (fig. 8.1), it is observed that the Q-S response has the usual high 1st harmonic content, whereas the unsteady response gives more important 2nd harmonic content, though they both have approximately the same coning angle. This can be attributed to the fact that in the Q-S theory, the blade flap forcing terms

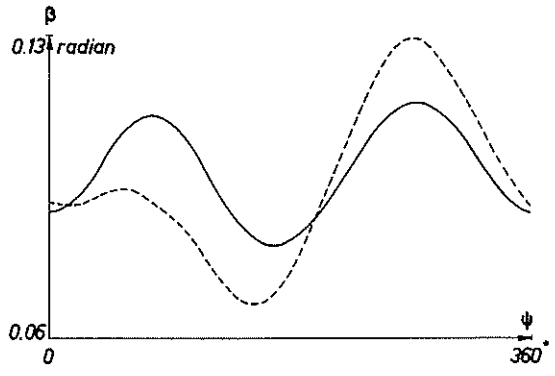

Fig. 8.1 : Blade flapping periodic response : ——— unsteady calculation ----- quasi-unsteady calculation

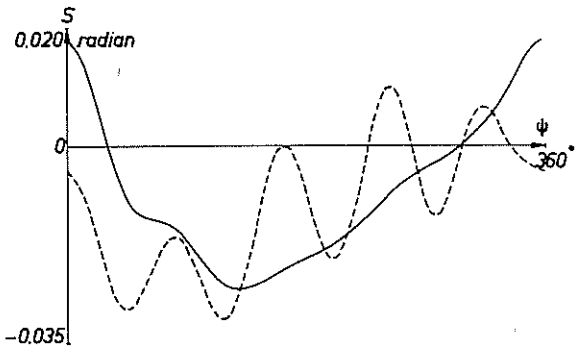

Fig. 8.2 : Blade torsional periodic response : ——— unsteady calculation ----Quasi-unsteady calculation

Fig. (8.3)

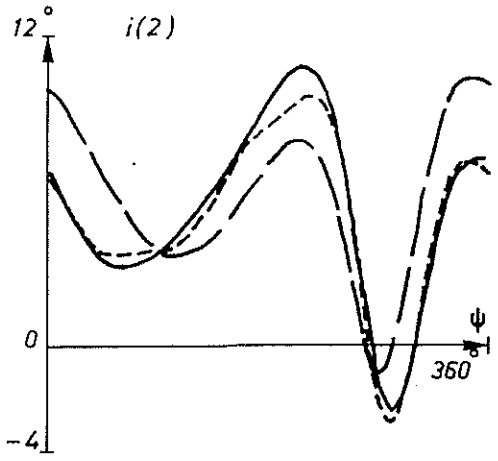

Fig. (8.4)

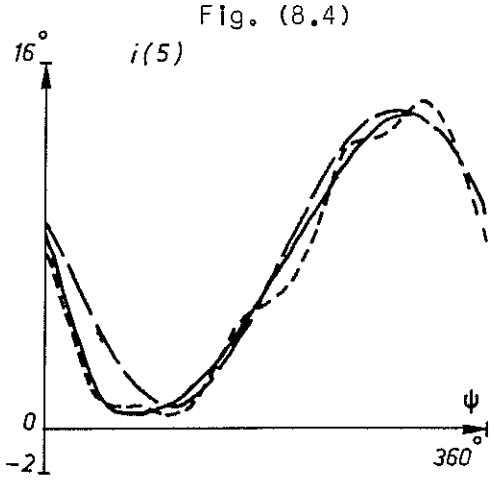

Fig. (8.5)

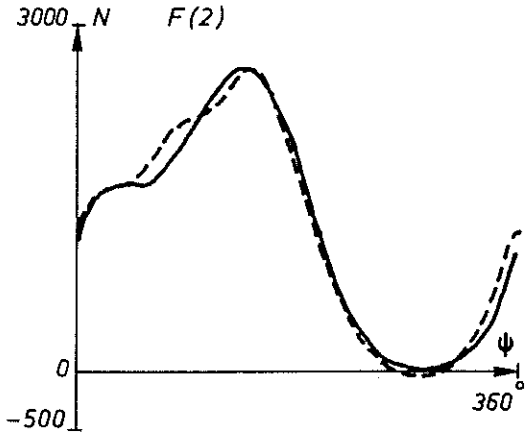

Fig. (8.6)

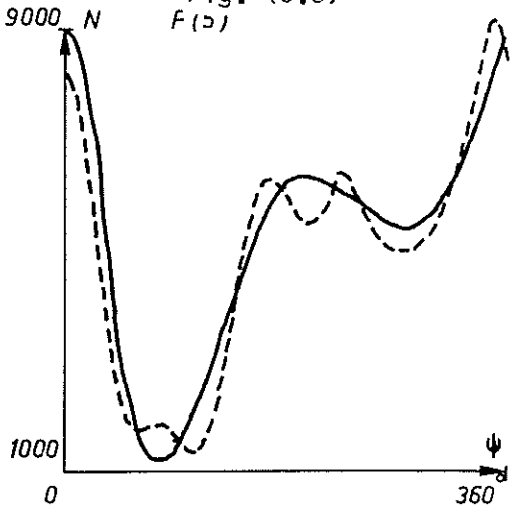

Fig. (8.7)

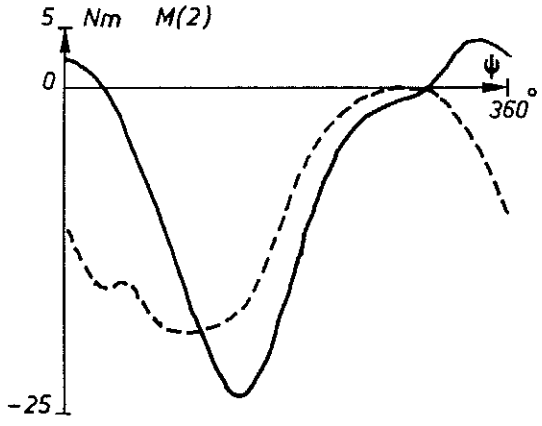

Fig. (8.8)

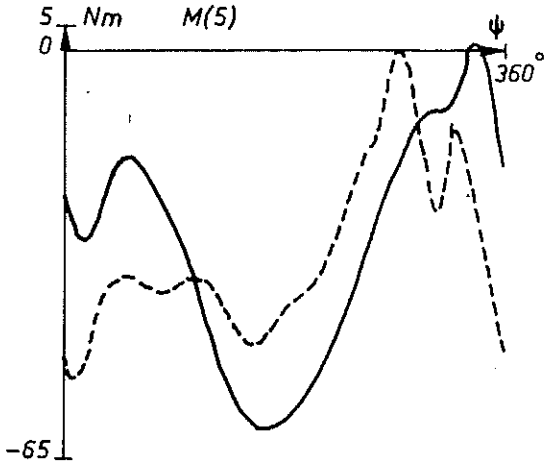

Fig.(8.3)-Fig. (8.8) : Blade incidence i, normal lift force F, and pitching moment M periodic response: _____ Unsteady calculation;---- Quasi-steady calculation;— — linearized incidence

consist mainly of the cyclic pitch excitation (equ. 2.5), and of the static lift function. In observing that at this flight speed where stall is not yet predominant, the static lift is mostly linear and hence the forcing function is mainly of the 1st harmonic. The higher harmonic contents in the unsteady calculation are consequence of stronger unsteady aeroelastic couplings. In both cases, the magnitudes of the blade flap harmonics are seemingly small, this being due to the input of the rotor shaft tilt angle of 5.5°.

As for the torsional responses α, fig. (8.2) ; it is known that the airfoil section static pitching moment curve presents abrupt break long before the static lift stall, the Q-S torsional moment forcing function is thus of high harmonics. Furthermore, there being no aerodynamic pitching moment damping in the Q-S calculation, the Q-S torsional response is then of the same nature as the forcing function.

The unsteady torsional response, however, is seen to be greatly filtered. The filtering could be the result of the high aerodynamic pitching moment damping and the effect of time delay.

Fig. (8.5) through fig. (8.8) present the comparisons of the normal lift forces F and the pitching moments M between the Q-S and the unsteady calculations. It is observed that the lift forces are quite insensitive to unsteady effects, while for approximately similar incidence evolutions, the difference between the two pitching moments are much more significant.

CONCLUSION

A single blade analysis for a helicopter rotor in hover and in forward flight has been developed, in which the unsteady aerodynamics was described by the ONERA 2-D dynamic stall model. It is considered that though the rotor mechanical system is greatly simplified, the present analysis is sufficient for the study of phenomena such as the stall flutter and subharmonic oscillation encountered by helicopters at high flight speeds.

As a consequence of the particularity of the aerodynamic model, the problem involves, apart from structural variables, additional aerodynamic degrees of freedom. The formulation leads to a set of linearized differential equations with periodic coefficients.

The stability of the aeroelastic system has been studies by the Floquet theory. It has been shown that subharmonic oscillation and almost periodic oscillation of the Floquet modes can readily occur. While it is generally admitted that responses of the form of subharmonic oscillation are due to non-linearities in the governing equations, the present study shows that this feature can also be attributed to the properties of the linear periodic differential equations, where the situation may be close to that of instability.

Comparisons of the periodic responses for both the quasi-steady and the unsteady calculations have also been shown. It is observed that while the blade normal lift force distribution is quite insensitive to unsteady effects, the blade aerodynamic pitching moment and the torsional response are subjected to more influence of the unsteady aerodynamic pitching moment damping and time delay effects.

The introduction of the blade flap and lead-lag elastic deformations should present no difficulty in principle by a modal superposition of the blade's normal modes. The effect of the C.G. offset with respect to the pitch or torsional axis can also be incorporated with no greater inconvenience. It remains to take into account by the aerodynamic model the large variation of the blade Mach number to include the compressibility effect. These will be attemped in future works.

REFERENCES

1. R. Dat, Aérodynamique instationnaire des pales d'hélicoptères. Table ronde sur l'aérodynamique instationnaire de l'AGARD, Göttingen, 30 mai (1975)

2. J.J. Costes, Calcul des forces aérodynamiques instationnaires des pales d'hélicoptères. Recherche Aérospatiale (1972-2)

3. C.T. Tran, W. Twomey, R. Dat — Calcul des caractéristiques dynamiques d'une structure d'hélicoptère par la méthode des modes partiels. Recherche Aérospatiale (1973-6)

4. R. Dat, C.T. Tran, D. Petot — Modèle phénoménologique de décrochage dynamique sur profil de pale d'hélicoptère. XVI Colloque d'Aérodynamique Appliquée (AAAF), Lille, Novembre (1979)

5. C.T. Tran, D. Petot — Semi-empirical model for the dynamic stall of airfoils in view of the application to the calculation of responses of a helicopter blade in forward flight. Sixth European Rotorcraft and Powered Lift Aircraft Forum, Bristol, September (1980)

6. R.P. Coleman, A.M. Feingold, C.W. Stempin — Evaluation of the induced velocity field of an idealized helicopter rotor. NACA ARR n° L5E10 (1945)

7. D. Favier, J. Repont, C. Maresca — Profil d'aile à grande incidence animé d'un mouvement de pilonnement. XVI Colloque d'Aérodynamique Appliquée (AAAF). Lille, Novembre (1979)

8. R.L. Bisplinghoff, H. Ashley, R.L. Halfman — Aeroelasticity, Addison - Wesley Publishing Company, Inc. (1957)

9 M.C. Pease, III, Methods of matrix algebra. Academic Press Inc. (1965)

10 M. Roseau, *Vibration non linéaire et théorie de la stabilité.* Springer Tracts, Natural Philosophy, Vol. 8 (1966)

11 C.S. Hsu, On approximating a general linear periodic system. Journal of Mathematical Analysis and Applications. 45, 234-251 (1974)

12 P. Friedmann, L.J. Silverthorn — Aeroelastic stability of periodic systems with application to rotor blade flutter. AIAA/ASME/SAE, 15th Structures, Structural Dynamics and Materials Conference. AIAA Paper n° 74-417, April (1974).